Available online at www.tjnsa.com
J. Nonlinear Sci. Appl. 9 (2016), 4877–4887
Research Article

Journal of Nonlinear Science and Applications
Print: ISSN 2008-1898 Online: ISSN 2008-1901

A computational method for converter analysis using point symmetries

Richard O. Ocaya

Department of Physics, University of the Free-State, P. Bag X13 Phuthaditjhaba 9866, South Africa.

Communicated by A. Atangana

Abstract

The one-parameter point transformation method is applied to clarify the use of symmetries to describe the effects of additive uncertainties on the state-space solutions of an affine control system. The trajectory of the solution in the presence of general, bounded uncertainties gives an idea of system robustness. The boost converter is used for illustration. A specific symmetry is computed under uncertainties and its effects on a possible solution are investigated. A comparison of the method with other state-space methods shows that it is an excellent approach if developed further. ©2016 All rights reserved.

Keywords: Lie point symmetries, boost converter, robustness, state-space, infinitesimal generator.
2010 MSC: 93C55, 93C70, 70G65.

1. Introduction

Consider the affine control system

$$\dot{x} = a(x) + \sum_{i=1}^{m} b_i(x)u_i(t), \tag{1.1}$$

where $a, b_i : R^1 \times R^n$ are smooth functions and u denotes the m controls. The current work, presents an application of group theory in the form of Lie symmetries [5, 6] to investigate the effects of uncertainties, perturbations, and neglected dynamics on solutions of Eq. (1.1), applied illustratively to the particular case of the boost converter. There are currently state-space based methods that allow the behavior of a system solution to be evaluated in the presence of uncertainties. The common starting point for these methods

Email address: ocayaro@ufs.ac.za (Richard O. Ocaya)

Received 2016-07-30

relies on a reasonable linear time-invariant (LTI) models of the system. The generally nonlinear closed loop system is first linearized by some means and then placed into a state-space form, with the uncertainties bundled together into a single bounded perturbation matrix of suitable dimension. The analysis then applies worst-case variations of the matrix to determine the bounds of performance of the system, whereupon a robustness measure is possible. In the present paper, rather than define a perturbation matrix, the worst-case variations in the uncertainties are evaluated directly by their effects on the solution trajectory of the LTI form. The behavior of a given solution under the modified trajectory then gives an idea of the robustness of the system under the specified uncertainties. Generally, the computation of symmetries of a differential equation is motivated by the need to find an integrating factor that reduces the problem to quadratures [9]. The method expressed below, implies the extension of an averaged state-space solution under group transformation. Finally, the results of a symmetries computation are compared with results using the other computational methods. Here, the waveforms of the perturbation matrix are simulated in Matlab and then compared with component level simulation in PSpice. The symmetries method is shown to be an alternative approach.

2. Boost converter dynamical equations

Consider the boost converter in Fig. 1. The non-idealities r_L, r_C and i_g, model both parametric and load uncertainties.

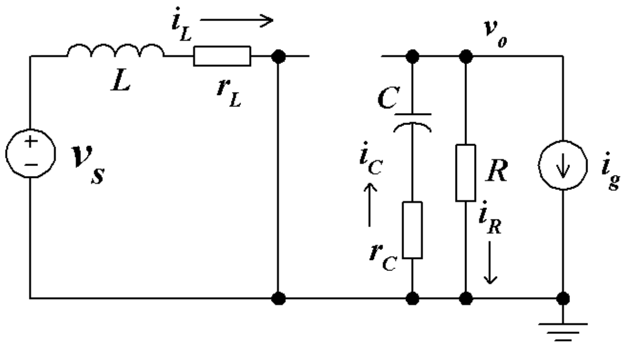

(a) During t_{on}. Switch is closed.

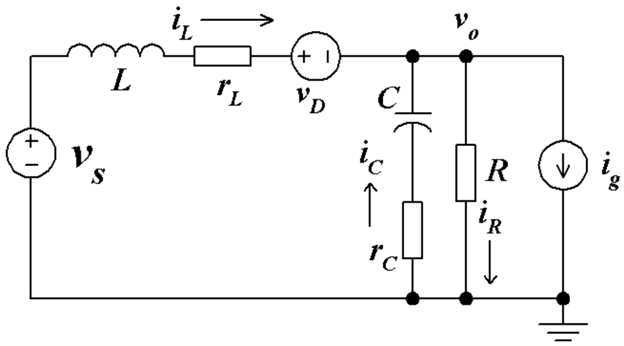

(b) During t_{off}. Switch is open.

Figure 1: Derivation of the boost converter circuit state-representation.

To arrive at a model, the system state equations are developed separately during each phase and then state-space averaged to a continuous small-signal model [11]. If the switch phases are denoted by $i = 1$ and $i = 2$ for switch closed and open, respectively, then during the two phases one can write

$$\begin{aligned} \dot{\mathbf{x}} &= \mathbf{A}_i\mathbf{x} + \mathbf{B}_i u \\ y &= \mathbf{C}_i\mathbf{x} + \mathbf{E}_i u, \end{aligned} \tag{2.1}$$

where $\mathbf{x} = [x_1 \;\; x_2]^T = [i_L \;\; v_C]^T$, $y = v_o$, and $u = [v_s \;\; i_g \;\; v_D]^T$. The matrices A_i, B_i, C_i and E_i for $i = (1, 2)$ are available for averaging, and convey system behavior and contain parametric uncertainties and other non-idealities as well. At steady state, quantities are $\mathbf{x} = [x_1 \;\; x_2]^T = [I_L \;\; V_C]^T$, $y = V_o$, and $u = [V_s \;\; I_g \;\; V_D]^T$, at duty cycle D.

2.1. The boost converter as a control affine system

Redefining the individual switch phase state equations in the form

$$\dot{x}_i = \mathbf{A}_i x_i + \mathbf{R}_i$$

for $i = 1, 2$, allows Eq. (2.1) to be rewritten as:

$$\dot{\mathbf{x}} = [(1-d)\mathbf{A}_1 + d\mathbf{A}_2]\mathbf{x} + [(1-d)\mathbf{R}_1 + d\mathbf{R}_2]. \tag{2.2}$$

Perturbing (2.2) around the equilibrium gives

$$\begin{aligned}\langle \dot{\mathbf{x}} \rangle &= \underbrace{\Big[\mathbf{A}_1 + (\mathbf{A}_2 - \mathbf{A}_1)D\Big]\hat{\mathbf{x}}}_{f(\hat{\mathbf{x}})} + \underbrace{\Big[(\mathbf{A}_2 - \mathbf{A}_1)X + (\mathbf{R}_2 - \mathbf{R}_1)\Big]\hat{d}}_{g(\hat{\mathbf{x}})} \\ \Rightarrow \quad \dot{\hat{\mathbf{x}}} &= f(\hat{\mathbf{x}}) + g(\hat{\mathbf{x}})u,\end{aligned}$$

where $u = \hat{d}$ is the single control. It is easy to show that

$$f(\hat{\mathbf{x}}) = \begin{bmatrix} -\frac{r_L(R+r_C)+r_C RD}{L(R+r_C)} & -\frac{RD}{L(R+r_C)} \\ \frac{RD}{C(R+r_C)} & -\frac{1}{C(R+r_C)} \end{bmatrix} \begin{bmatrix} x_1 \\ x_2 \end{bmatrix}$$

and

$$g(\hat{\mathbf{x}}) = \begin{bmatrix} \frac{-r_C R I_L - V_C R + R r_C i_g - V_D(R+r_C)}{L(R+r_C)} \\ \frac{R I_L}{C(R+r_C)} \end{bmatrix}.$$

In the absence of parametric uncertainty,

$$f(\hat{\mathbf{x}}) = \begin{bmatrix} -\frac{D}{L}x_2 \\ \frac{D}{C}x_1 - \frac{1}{RC}x_2 \end{bmatrix} \quad \text{and} \quad g(\hat{\mathbf{x}}) = \begin{bmatrix} -\frac{V_C+V_D}{R} \\ \frac{I_L}{C} \end{bmatrix}, \tag{2.3}$$

where

$$I_L = \frac{1}{D}\Big(\frac{V_C}{R} + I_g\Big), \quad V_C = \frac{V_s}{D} \ \text{ and } \ V_o = V_C.$$

Example 2.1. An idealized boost converter having V_o=48.0V, V_s=12.0V requires that D=0.75; for a 50 watts rated output with a constant load current I_g=0, then R=46.08 Ω.

2.2. *Existence of boost converter symmetries*

The behaviour of solutions under the one-parameter transformation can then be used to highlight the effects of parametric and other uncertainties on the system solution through its symmetries. The illustration of a symmetry method here is based on the observation that a reversible one-parameter transformation maps the generally nonlinear system to a linear and equivalent one (see [2]).

2.2.1. *Symmetries of the generalized control system*

Consider the generalized dynamic system

$$\dot{x} = f(t, x, u) \tag{2.4}$$

with state x and arbitrary control u.

The three-tangent vector fields (ξ, η, φ) of Eq. (2.4) lead to the symmetry generator

$$X = \xi(t,x,u)\partial_t + \sum_{i=1}^{n} \eta_i(t,x,u)\partial_{x_i} + \sum_{i=1}^{m} \varphi_j(t,x,u)\partial_{u_j} \tag{2.5a}$$

with respect to independent variable t. The first-order prolongation is

$$X^{(1)} = X + \sum_{i=1}^{n} \zeta_i(t,x,u,x',u')\partial_{x_i'} + \sum_{j=1}^{m} \psi_j(t,x,u,x',u')\partial_{u_j'} \tag{2.5b}$$

with the total derivative operator

$$D_t = \partial_t + \sum_{i=1}^{n} x' \partial_{x'_i} + \sum_{j=1}^{m} u' \partial_{u'_j}.$$

The functions ζ and ψ are calculated from

$$\zeta = D_t \eta - x' D_t \xi \qquad \text{and} \qquad \psi = D_t \varphi - u' D_t \xi.$$

Infinitesimal symmetries [3, 4] are also generated by the admission of $\hat{f} = \hat{f}(t, x, x', u, u')$, provided that

$$X^{(1)}(\hat{f}) = 0.$$

Consequently, a necessary and sufficient condition for the new coordinate system (in a form linear in u') is

$$\xi f_t + f_x \eta + f_u \varphi - \eta_t - \eta_x f - \eta_u u' + f(\xi_t + \xi_x f + \xi_u u') = 0. \tag{2.6}$$

Eq. (2.6) is reduced to the defining equations

$$\xi f_t + f_x \eta + f_u \varphi - \eta_t - \eta_x f + f \xi_t + f \xi_x f = 0, \tag{2.7a}$$

$$\eta_u - f \xi_u = 0. \tag{2.7b}$$

Eqs. (2.7) can be written in Lie bracket notation by noting firstly that Eq. (2.4) is a vector field with the form

$$F = \frac{\partial}{\partial t} + \sum_{i=1}^{n} f_i \frac{\partial}{\partial x_i} \tag{2.8a}$$

for $i = (1, 2, \ldots, n)$. Secondly, the most general infinitesimal generator H can be defined by

$$H = \xi \frac{\partial}{\partial t} + \sum_{i=1}^{n} \eta_i \frac{\partial}{\partial x_i}.$$

Both F and H are independent of the controls, i.e., $\partial_u F = \partial_u H = 0$. Eq. (2.5a) then becomes

$$X = H + \sum_{j=1}^{m} \varphi_j \partial_{u_j}.$$

Similarly, defining a Lie bracket F_j such that

$$F_j = [\partial_{u_j}, F] = \left[\frac{\partial}{\partial u_j}, F\right], \qquad \text{for } j = 1, 2, \ldots, m,$$

allows Eq. (2.7a) to be written as

$$[F, H] - F(\xi) F = \sum_{j=1}^{m} \varphi_j F_j. \tag{2.8b}$$

Similarly, Eq. (2.7b) becomes

$$\left[\frac{\partial}{\partial u_j}, H\right] - \frac{\partial \xi}{\partial u_j} F = 0. \tag{2.8c}$$

2.2.2. Symmetries of the affine control system

Consider the control affine system

$$\dot{x} = a(t, x) + \sum_{j=1}^{m} b(t, x) u_j \equiv f(t, x, u), \quad x \in R^n \tag{2.9}$$

with state x, control u, independent variable t and continuously differentiable functions a and b. Then provided that $f_i = A_i + B_i u_i$, it is possible to define two control-independent vector fields A and B ($\partial_u A{=}\partial_u B_j{=}0$) for Eq. (2.9) such that

$$A = \frac{\partial}{\partial t} + \sum_{i=1}^{n} a_i \frac{\partial}{\partial x_i}, \quad \text{and} \quad B_j = \sum_{i=1}^{n} b_{ij} \frac{\partial}{\partial x_i}$$

for $j = 1, 2, \ldots, m$. Eq. (2.8a) becomes

$$F = A + \sum_{j=1}^{m} u_j B_j.$$

This allows Eqs. (2.8b) and (2.8c) to be written as:

$$[F, H] - F(\xi)F = \sum_{j=1}^{m} \varphi_j B_j,$$

$$\left[\frac{\partial}{\partial u_k}, H\right] - \frac{\partial \xi}{\partial u_k}\left(A + \sum_{j=1}^{m} u_j B_j\right) = 0$$

for $k = 1, 2, \ldots, m$ (see [7]). Let $\mathcal{B}$ define the set of all vector fields with basis B_j. Then the commutators are such that

$$[F, H] = [A, H] + \sum^{m} [u_j B_j, H] \in \mathcal{B}.$$

Similarly,

$$F(\xi)F = A(\xi)A + \underbrace{\sum^{m} u_j A(\xi) B_j}_{\text{explicitly in } \mathcal{B}} + \sum^{m} u_j B_j(\xi) A + \underbrace{\sum_{j,k=1}^{m} u_j u_k B_j(\xi) B_k}_{\text{explicitly in } \mathcal{B}} \in \mathcal{B}.$$

Combining these equations gives

$$[F, H] - F(\xi)F = [A, H] + \sum^{m} [u_j B_j, H] - A(\xi)A - \sum^{m} u_j A(\xi) B_j - \sum^{m} u_j B_j(\xi) A$$
$$- \sum_{j,k=1}^{m} u_j u_k B_j(\xi) B_k \in \mathcal{B}.$$

This leads to a form that is linear in the controls u_j, i.e.,

$$[A, H] - A(\xi)A - \sum_{j=1}^{m} u_j \underbrace{\Big\{B_j(\xi)A - [B_j, H]\Big\}}_{A_j} = \sum_{j=1}^{m} u_j A_j \in \mathcal{B}.$$

In addition, it can be seen that

$$[A, H] - A(\xi)A \in \mathcal{B}, \quad \text{and} \quad \sum_{j=1}^{m} u_j \Big\{B_j(\xi)A - [B_j, H]\Big\} \in \mathcal{B}.$$

2.2.3. Symmetries of the affine system with scalar control

The following examples are presented for scalar control, i.e., m=1.

Example 2.2. If the vector field H is a true symmetry of the affine dynamic control system:

$$\dot{x} = a(t, x) + b(t, x)u,$$

then it satisfies the conditions

$$[A,H]-A(\xi)\in\mathcal{B},\qquad [B,H]-B(\xi)\in\mathcal{B},\qquad \left[\frac{\partial}{\partial u},H\right]-\frac{\partial\xi}{\partial u}(A+uB)=0$$

for each A and B, where

$$A=\frac{\partial}{\partial t}+\sum_{i=1}^{n}a_i(t,x)\frac{\partial}{\partial x_i},\quad\text{and}\quad B=\sum_{i=1}^{n}b_i(t,x)\frac{\partial}{\partial x_i}.$$

According to [10], if the vector fields A and B possess the iterated Lie brackets $\mathrm{ad}_A^0 B,\ \mathrm{ad}_A^{r+1}B$ for $r>1$ with dimension n, then the system satisfies the condition of rank controllability. In other words, the series

$$\mathrm{ad}_A^0 B,\ \mathrm{ad}_A^1 B,\ \ldots,\ \mathrm{ad}_A^{n-1}B$$

have rank n.

Example 2.3. Suppose that the n-dimensional affine system with the symmetry generator

$$X=\xi(t,x,u)\partial_t+\sum_{i=1}^{n}\eta_i(t,x,u)\partial_{x_i}+\sum_{i=1}^{m}\varphi_j(t,x,u)\partial_{u_j}$$

satisfies the rank controllability condition at the point (t,x). Then the vector field H is a symmetry of X in the neighborhood of (t,x) iff

$$H=\xi A+\sum_{i=0}^{n-1}h_i\mathtt{ad}_A^i B$$

under the necessary and sufficient conditions that

$$\begin{aligned}
&A(h_j)=-h_{j-1}-h_{n-1}\alpha_j,\quad j=1,2,\ldots,n-1,\\
&B(h_j)+\sum_{k=1}^{n-1}\beta_{jk}h_k=0,\quad j=2,3,\ldots,n-1,\\
&\xi=B(h_1)+\sum_{k=1}^{n-1}\beta_{1k}h_k.
\end{aligned}$$

The coefficients α_j and β_{jk} are functions of (t,x) and are calculated from the iterated Lie series:

$$\mathtt{ad}_A^n B=\sum_{i=0}^{n-1}\alpha_i\mathtt{ad}_A^i B,\quad\text{and}\quad [B,\mathtt{ad}_A^k B]=\sum_{j=0}^{n-1}\beta_{jk}\mathtt{ad}_A^j B$$

for $k=1,2,\ldots,n-1$.

Example 2.4. Consider a two-state affine system that is rank-controllable and has scalar control. Thus $n=2$ and $m=1$. It follows that

$$H=\xi A+\sum_{i=0}^{1}h_i\mathtt{ad}_A^i B=\xi A+h_0B+h_1[A,B],$$

where

$$A=\frac{\partial}{\partial t}+\sum_{i=1}^{2}a_i(t,x)\frac{\partial}{\partial x_i}\quad\text{and}\quad B=\sum_{i=1}^{2}b_i(t,x)\frac{\partial}{\partial x_i}.$$

In $A(h_i)$ and $B(h_j)$, $j=1$, hence $A(h_1)=-h_0-h_1\alpha_1$, or $h_0=-A(h_1)-h_1\alpha$. Also $\xi=B(h_1)+\beta_{11}h_1$.

2.2.4. Symmetries of a two-dimensional affine system with scalar control

Example 2.5. If $n = 2$ and $m = 1$ then the affine system in Eq. (2.9) has the most general infinitesimal generator

$$H = \xi A + hB \tag{2.10}$$

for an arbitrary function h=$h(u)$.

Proof. $\mathtt{ad}^0_A B$=$[A, B]$=0; also, $\mathtt{ad}^2_A B$=$\alpha_0 \mathtt{ad}^0_A B$+$\alpha_1 \mathtt{ad}^1_A B$; $\mathtt{ad}^1_A B$=0. Since $B \neq 0$, it follows that α_0 vanishes but not necessarily α_1. Thus $H = \xi A + h_0 B$. Putting h_0=h completes the proof. □

Example 2.5 implies that by equation (2.8c) one can conclude that

$$[\partial_u, \xi A + hB] - \xi_u(A + uB) = 0,$$

which is reduced to the selection condition,

$$h_u - u\xi_u = 0. \tag{2.11}$$

Example 2.6. Consider a nominal 50 watt boost converter with L=250μH, C=100μF, R=46.08Ω and D=0.75; the nominal output and input voltages are 48.0V and 12.0V, respectively. Then, Eq. (2.3) gives

$$f(x) = 10^3 \begin{bmatrix} -0.00 & -3.00 \\ +7.50 & -0.22 \end{bmatrix} \mathbf{x}, \qquad \text{and} \qquad g(x) = 10^4 \begin{bmatrix} -0.00 \\ +4.17 \end{bmatrix}.$$

2.3. Application of the generated symmetries

The condition expressed by Eq. (2.11) is met by infinitely many symmetry-determining functions h and ξ. Some possible (h, ξ) combinations are $(2u, u^2)$, $(u^2/2, u)$, $(u, \ln u)$. Even the simple boost converter has infinitely many possible symmetries.

Example 2.7. For the system in Example 2.6, the functions h=$2u$ and ξ=u^2 produce a valid symmetry of the form (2.10). The coefficients a_i and b_i for i=1,2 are determined from $f(x)$ and $g(x)$ in Example 2.6, i.e.,

$$a_1 = -3000x_2,\ a_2 = 7500x_1 - 220x_2,$$

and

$$b_1 = 0,\ b_2 = 41700.$$

The most general infinitesimal generator is then

$$H = u^2\partial_t - 3000x_2u^2\partial_{x_1} + (7500x_1 - 220x_2)u^2\partial_{x_2} + 83400u\partial_{x_2}.$$

In [12], it is shown that if $y = f(\varphi)$ is an arbitrary solution of the ODE, then invariance in the group implies that new solutions $\hat{y}(\hat{\varphi})$ can be found under the one-parameter ε, such that

$$(\hat{y}, \hat{\varphi}) = e^{\varepsilon H}(y, \varphi). \tag{2.12}$$

In the case of the affine system we have, $\varphi = (t, \mathbf{x}, u)$.

Example 2.8. As an illustration, suppose that the output voltage x_2 is given by

$$x_2(t) = V_C(1 - e^{-\alpha t})$$

for α=100 and V_C=48.0V, as shown in Fig. 2(b). Suppose that the trajectory of x_2 under the action of the symmetry H in equation (2.12) can be found.

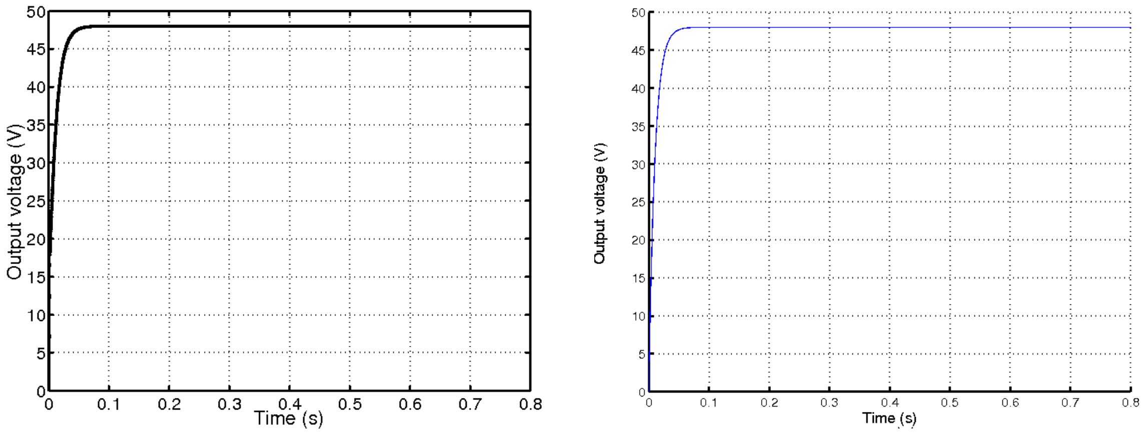

(a) Nominal Simulink output for Fig.4. (b) Possible nominal solution, Eq.(2.13).

Figure 2: Estimated output voltage (the state variable x_2) in the closed-loop solution trajectory.

New solutions can be computed using Eq. (2.12), i.e.,

$$\hat{x}_2 = e^{\varepsilon H} x_2.$$

The action of H can be investigated termwise, i.e., firstly terms of $\partial_t x_2$, then $\partial_{x_1} x_2$ and finally $\partial_{x_2} x_2$. Eq. (2.13) is explicitly independent of x_1 so that $\partial_{x_1} x_2$ vanishes. Therefore, the action of H can be resolved into two independent actions, namely that on the time axis and that on the x_2 axis. For action along the time axis, $H \equiv u^2 \partial_t$, so that

$$\begin{aligned} e^{\varepsilon H} x_2 &= \Big[1 + \varepsilon H + \frac{(\varepsilon H)^2}{2!} + \frac{(\varepsilon H)^3}{3!} + \dots\Big] x_2 \\ &= x_2 + \varepsilon H x_2 + \frac{\varepsilon^2 H(Hx_2)}{2!} + \frac{\varepsilon^3 H(H(Hx_2))}{3!} + \dots. \end{aligned} \tag{2.13}$$

But $Hx_2 {=} \alpha u^2 V_C e^{-\alpha t}$, so that

$$H^n x_2 = (-1)^{n+1} (\alpha u^2)^n V_C e^{-\alpha t}.$$

Hence

$$\begin{aligned} \hat{x}_2 = e^{\varepsilon H} x_2 &= V_C - V_C e^{-\alpha t}\Big[1 - (\varepsilon \alpha u^2) + \frac{(\varepsilon \alpha u^2)^2}{2!} - \frac{(\varepsilon \alpha u^2)^3}{3!} + \dots\Big] \\ &= V_C - V_C e^{-\alpha t} e^{-\varepsilon \alpha u^2} \\ &\Rightarrow \hat{x}_2 = V_C\Big[1 - e^{-\alpha(t + \varepsilon u^2)}\Big]. \end{aligned} \tag{2.14}$$

Eq. (2.14) is a symmetry of Eq. (2.9) that achieves a scaling translation of the time axis since $\hat{x}_2 {=} x_2$ when $\varepsilon{=}0$. The transformation does not affect the magnitude of x_2.

For action along the x_2 axis, $H \equiv [(7500x_1 - 220x_2)u^2 + 83400u]\partial_{x_2}$, so that

$$\begin{aligned} e^{\varepsilon H} x_2 &= \Big[1 + \varepsilon H + \frac{(\varepsilon H)^2}{2!} + \frac{(\varepsilon H)^3}{3!} + \dots\Big] x_2 \\ &\Rightarrow \hat{x}_2 = x_2 + \varepsilon[(7500x_1 - 220x_2)u^2 + 83400u]. \end{aligned} \tag{2.15}$$

Eq. (2.15) is another symmetry of Eq. (2.9) that also scales and translates the output amplitude since $\hat{x}_2 {=} x_2$ when $\varepsilon{=}0$. Fig. 3 shows the effect that the symmetry H has on the time axis and on the output voltage. This example shows that the effects of parametric uncertainty are absent from the time-axis calculation, but are present in the x_2 transformation.

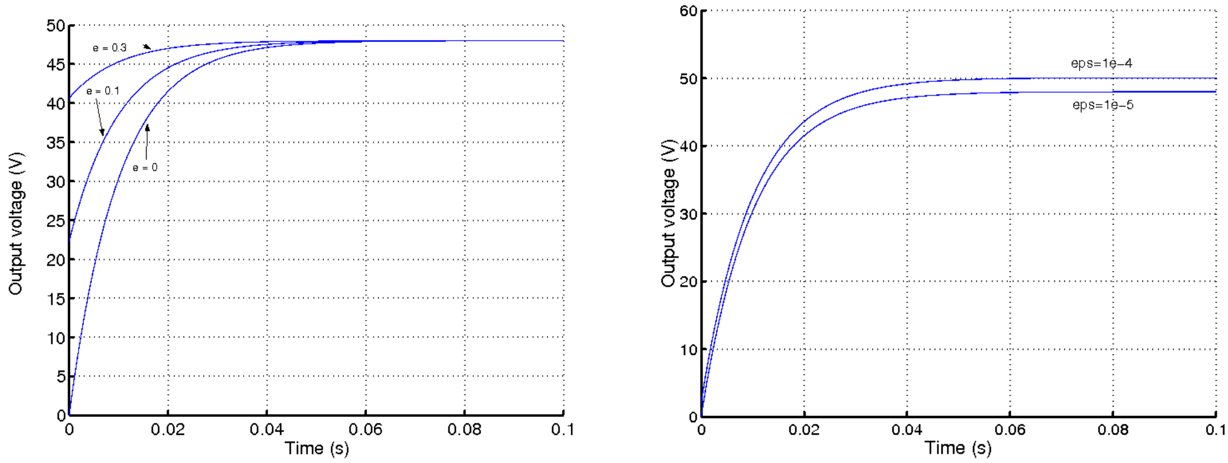

(a) The effect of timing element uncertainties on output rise-time.

(b) The effect of input voltage disturbance on output amplitude.

Figure 3: The transformation of the symmetries in Eqs. (2.14) and (2.15) on a solution x_2. The nominal voltage magnitude of x_2 is 48.0V.

3. The effect of perturbations on affine symmetries

The use of symmetries to investigate the effects of general perturbations could enhance the understanding of these effects on a system. The task of developing analytical tools using symmetries is clearly not trivial. However, the generality of symmetries enables a large class of uncertainty to be factored into the analysis, where the treatment of generalized perturbations is reduced to a differential inclusion [1].

Example 3.1. Suppose that Eq. (2.9) has norm-bounded additive uncertainties α, β and γ that represent matched uncertainties in a, b and u, respectively. Then the idealized system

$$\dot{x} = f(t,x) + \sum^{m} b_i(t,x)u_i(t,x)$$

can be written in a form with uncertainties

$$\begin{aligned}\dot{x} &= (a+\alpha a) + \sum^{m}(b_i+\beta_i b_i)(u_i+\gamma_i u_i)\\ &= \underbrace{\Big(a+\sum^{m} b_i u_i\Big)}_{\text{idealized system}} + \underbrace{\Big(\alpha a+\sum^{m}\delta_i b_i u_i\Big)}_{\text{perturbation}}\\ &= f(t,x,u) + h(\alpha,\delta,t,x,u)\\ &= h(t,x,u,\alpha,\delta),\end{aligned} \tag{3.1}$$

where $\delta_i = (\gamma_i, \beta_i)$. Hence the affine system with additive uncertainties becomes a differential inclusion with the uncertainties lumped together into the inclusion function.

In summary, the differential inclusion function $h(\alpha,\delta,t,x,u)$ lumps all the generalized uncertainties together, outside of the idealized system while retaining the additive perturbative character.

4. Comparison with a Simulink result

A brief comparison of the results obtained using the symmetries method with Simulink is achieved using the Simulink model shown in Fig. 4. The block labeled P_CL denotes the optimal closed loop system with a minimized $\mathcal{H}_\infty$ controller. For the sake of simplicity, the model is grouped into the subsystem in Fig. 4 with bounded additive perturbations applied singly or simultaneously. In addition, all the inherent optimized weights and pre-filters have been included [8]. In the interest of illustration of the principle, only the effect of supply-line uncertainty (labeled "noise" in Fig. 4) is considered.

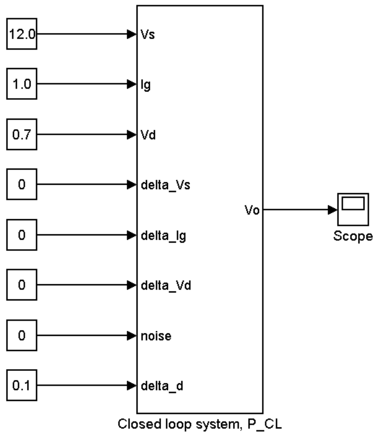

Figure 4: Closed loop weighted disturbance model subsystem for Simulink simulation.

Fig. 5 illustrates the upper and lower boundaries of the output in the presence of a sufficiently strong disturbance applied on the input source, V_s. It compares well with the symmetries result shown in Fig. 3(b). One apparent importance of the symmetries method then is the establishment of the bounds of trajectory variation in the presence of bounded perturbations.

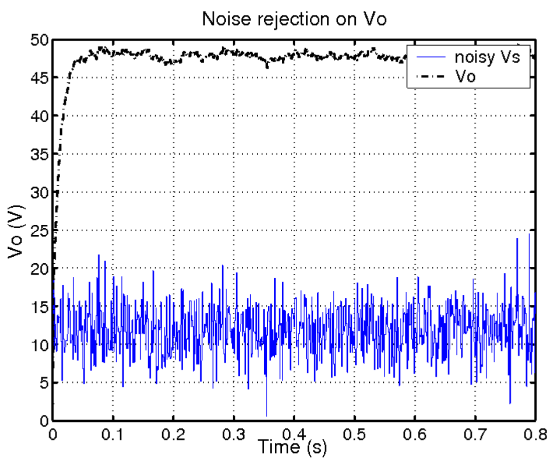

Figure 5: Uncertainty rejection using band-limited white noise of sample time = 0.001s and noise power 0.001 applied on V_s.

5. An alternative symmetries approach for uncertain systems

Eq. (3.1) has two additional independent variables (namely α and δ) over Eq. (2.9). Therefore, the uncertain system will have two additional tangent vectors in addition to (ξ,η,φ). Thus the control system

$$\dot{x} = f(t, x, u, \alpha, \delta)$$

with infinitesimal generators $X^{(n)}$ (in the form of Eq. (2.5b)), expresses matched uncertainties in the arguments of function f.

6. Conclusions

This paper has outlined a computational method using the symmetries to evaluate the effects of uncertainties on generalized dynamical systems. It outlines the approach for the affine control system with scalar control and additively applied uncertainties. Illustrations are done using the particular case of the boost converter. The symmetries are shown to transform the state and independent variables as expected, thereby providing a means to quantify these effects. An apparent drawback of the method is the amount of computation required as a price of its generality. This fact above all else, has meant that symmetry methods are generally avoided. The examples provided in the paper highlight that the method can be very useful if the complexity is acceptable.

References

[1] A. Cellina, *A view on differential inclusions*, Rend. Semin. Mat. Univ. Politec. Torino, **63** (2005), 197–209. 3
[2] R. D. Costin, *Nonlinear perturbations of Fuchsian systems: corrections and linearization, normal forms*, Nonlinearity, **21** (2007), 2073–2082. 2.2
[3] P. E. Hydon, *Symmetry methods for differential equations*, A beginner's guide, Cambridge Texts in Applied Mathematics, Cambridge University Press, Cambridge, (2000). 2.2.1
[4] P. E. Hydon, *An introduction to symmetry methods in the solution of differential equations that occur in Chemistry and Biology*, Int. J. Quantum Chem., **106** (2006), 266–277. 2.2.1
[5] N. H. Ibragimov, *Elementary Lie group analysis and ordinary differential equations*, Wiley Series in Mathematical Methods in Practice, John Wiley & Sons, Ltd., Chichester, (1999). 1
[6] N. H. Ibragimov, *Introduction to modern group analysis*, Ufa, (2000). 1
[7] A. N. Kanatnikov, A. P. Krishchenko, *Symmetry of affine systems*, Methods of analysis of nonlinear systems, Comput. Math. Model., **9** (1998), 64–75. 2.2.2
[8] A. Lanzon, *Weight optimization in $\mathcal{H}_\infty$ loop shaping*, Automatica, **41** (2005), 1201–1208. 4
[9] P. G. L. Leach, S. É. Bouquet, *Symmetries and integrating factors*, J. Nonlinear Math. Phys., **9** (2002), 73–91. 1
[10] H. Nijmeijer, A. van der Schaft, *Nonlinear dynamical control systems*, Springer-Verlag, New York, (1990). 2.2.3
[11] K. Ogata, *Modern control engineering, 3rd edition*, Prentice Hall, USA, (1997). 2
[12] P. J. Olver, *Applications of Lie groups to differential equations*, Graduate Texts in Mathematics, Springer-Verlag, New York, (1986). 2.3